J. Fluid Mech. (1981), vol. 110, pp. 171–194
Printed in Great Britain

Turbulence structure of a reattaching mixing layer

By C. CHANDRSUDA AND P. BRADSHAW
Department of Aeronautics, Imperial College, London

(Received 6 August 1980)

Hot-wire measurements of second- and third-order mean products of velocity fluctuations have been made in the flow behind a backward-facing step with a thin, laminar boundary layer at the top of the step. Measurements extend to a distance of about 12 step heights downstream of the step, and include parts of the recirculating-flow region: approximate limits of validity of hot-wire results are given. The Reynolds number based on step height is about 10^5, the mixing layer being fully turbulent (fully three-dimensional eddies) well before reattachment, and fairly close to self-preservation in contrast to the results of some previous workers. Rapid changes in turbulence quantities occur in the reattachment region: Reynolds shear stress and triple products decrease spectacularly, mainly because of the confinement of the large eddies by the solid surface. The terms in the turbulent energy and shear stress balances also change rapidly but are still far from the self-preserving boundary-layer state even at the end of the measurement region.

1. Introduction

This paper is one of a series on complex turbulent flows, defined as shear layers which are perturbed by interaction with another turbulence field or by externally imposed distortion. For a general review see Bradshaw (1975); the research programme of which the present paper forms a part is described by Bradshaw (1976, 1978). The reattachment of a mixing layer at the end of a separation bubble is an example of a flow in which the shear layer changes its species (i.e. its name); after reattachment to the surface, the mixing layer is called a boundary layer, although it is clear that relaxation from the turbulence structure typical of a mixing layer to that typical of a boundary layer will not be instantaneous. A species change (from boundary layer to mixing layer) occurs at the separation point also: in the present experiments the ratio of initial boundary-layer thickness to step height was made as small as possible, about 0·04 (an 'overwhelming perturbation' in the sense of Bradshaw & Wong 1972) so as to uncouple the two changes of species as far as possible. In view of the considerable controversy about persistence of the effect of initial conditions on mixing-layer development (e.g. Wygnanski *et al.* 1979), we took some care to run the present experiment at a high-enough Reynolds number to ensure that the mixing layer was fully developed before reattachment, as far as it was possible to judge this in a non-self-preserving flow.

The present study, a continuation of that of Bradshaw & Wong, was performed on a simple but realistic geometry, the low-speed flow over a backward-facing step with a thin laminar boundary layer at separation (in a plane mixing layer, full development is reached more quickly when the initial boundary layer is laminar than when it is turbulent, according to the measurements of Bradshaw 1966, and Hussain & Zedan 1978). The results are presented in more detail by Chandrsuda (1976). Because the separation line is fixed at the top of the step the flow is more steady than in other forms of separation bubble, with no trace of low-frequency buffeting. The ratio of wind tunnel width to step height was 15 to 1, above the value of 10 to 1 recommended by Brederode (1975) for the avoidance of significant three-dimensional effects near the centre plane. The object was to study the initial stages of relaxation after reattachment, rather than the separated flow region itself, and so hot-wire anemometers were used for turbulence measurements, accepting that the results were likely to be inaccurate in regions of small or negative mean velocity. The final application of the results is to calculation methods based on Reynolds-stress transport equations, and the measurements include enough terms in the transport equations for turbulent energy and shear stress for the remaining terms to be deduced by difference. In a further experiment (Wood 1980) we have studied the 'reattachment' of a mixing layer to a splitter plate placed parallel to the flow on the *high* velocity side of the mixing layer; this allows the influence of a solid surface as such (principally the imposition of the normal velocity constraint $v = 0$) to be studied in the absence of the strong pressure gradients that occur in the present flow.

The most noticeable features of the present results are the rapid decrease in all Reynolds stresses in the reattachment region, and the large changes in shape of the profiles of triple-velocity products. This change in shape seems to be the direct result of the normal velocity constraint at the wall, resulting in distortion of the large eddies by effectively irrotational mechanisms. Similar large changes in triple products were noticed in the latter stages of the mixing layer investigated by Castro & Bradshaw (1976), and indeed significant changes in triple products occurred in the latter experiment before the mixing layer had reached the solid surface. Wood also found decreases in triple products, but not the decrease in Reynolds stresses found in the present reattaching mixing layer. Since turbulent transport by triple products is a very significant part of the Reynolds stress balance in a mixing layer, it has to be modelled with reasonable accuracy in calculation methods, and the implication of these results is that algebraic relations between the triple products and the Reynolds stresses (or their gradients) are likely to be inadequate for strongly perturbed flows, making it necessary to use transport equations for the triple products. A similar conclusion was reached by Smits, Young & Bradshaw (1979) and by Smits, Eaton & Bradshaw (1979) on the basis of experiments on attached turbulent boundary layers perturbed by strong longitudinal curvature and/or lateral divergence.

Bradshaw & Wong (1972) reviewed existing experiments on the low-speed flow downstream of steps, fences and similar obstacles; more recent work includes that of di Gesso (1975), Eaton & Johnston (1980), and Etheridge & Kemp (1978). Almost the only high-speed experiment in which turbulence measurements were made is that of Gaviglio *et al.* (1977) and no experiment at any speed has included sufficient detail for balances of the Reynolds stresses to be deduced. Furthermore, the large streamwise variations of turbulence intensity in the mixing layer well upstream of reattachment, observed in some of the previous experiments, suggests that the flow was still strongly influenced by the conditions existing at the separation point. The present, more detailed, measurements of the reattachment of an apparently well-behaved mixing layer give a much fuller picture of the flow development, in spite of the

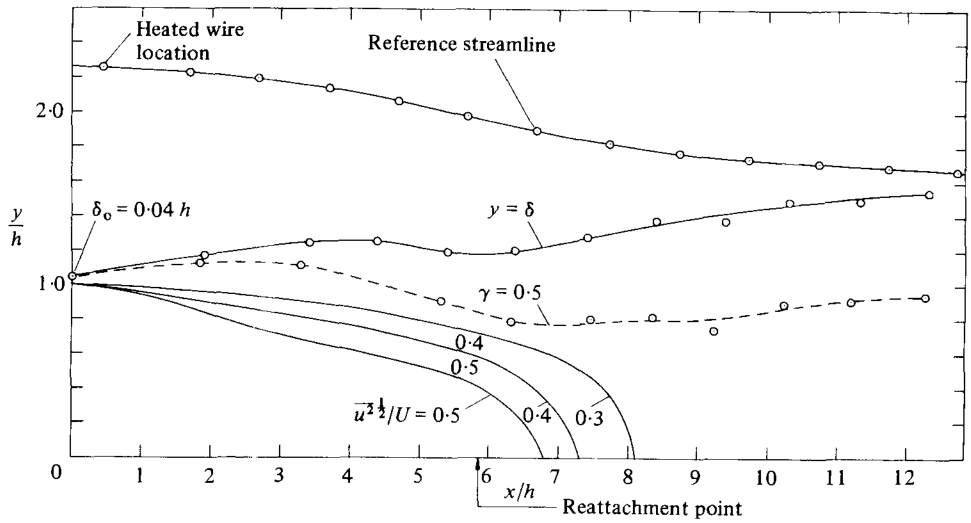

FIGURE 1. Backstep configuration, showing approximate contours of turbulence intensity. Hot-wire results dubious if $\overline{u^2}^{\frac{1}{2}}/U > 0{\cdot}3$, and only of qualitative use if $\overline{u^2}^{\frac{1}{2}}/U > 0{\cdot}5$. Vertical scale enlarged 2·5 times. Reattachment position from surface oil-flow observation.

inevitable unreliability of the hot-wire results in the recirculating region and near the reattachment point. There remains a need for similarly extensive measurements using a laser-Doppler anemometer.

2. Apparatus and techniques

The measurements were made in an open-circuit blower wind tunnel (Bradshaw 1972) with a working section 762 mm wide and initially 127 mm high, with a backward-facing step of height 51 mm on the floor immediately downstream of the contraction. The roof was inclined downwards at 1·7° downstream of the step to simulate a streamline in an infinitely high tunnel. Measurements were made up to a distance of about 760 mm (15 step heights) behind the step. All measurements were made at a flow speed over the top of the step, U_{ref}, of 31·5 m s^{-1}; the boundary layer 0·8 mm upstream of the step edge was laminar and 2 mm thick, implying a momentum thickness θ of about 0·2 mm, $U_{\text{ref}}\,\theta/\nu = 400$. The velocity profile at this point was still close to the Blasius shape, acceleration upstream of the step being negligible.

Mean velocity profiles were measured with a plane-ended circular Pitot tube of 1 mm outside diameter in conjunction with a disk static probe, as described by Bryer & Pankhurst (1971), of 6·4 mm diameter and 0·9 mm thickness. Pitot measurements were corrected for probe displacement effects, but no corrections were made for the effect of turbulence on the readings, and a significant part of the measured static pressure variation across the shear layer is attributable to effects of turbulence on the static pressure probe (Christiansen & Bradshaw 1981). A special kind of surface pressure 'tube', similar to that used by Sivasegaram (1971) and consisting of a spanwise slot with the aft lip about 0·05 mm higher than the forward lip, was used to measure local skin friction; the device was calibrated against a set of Preston

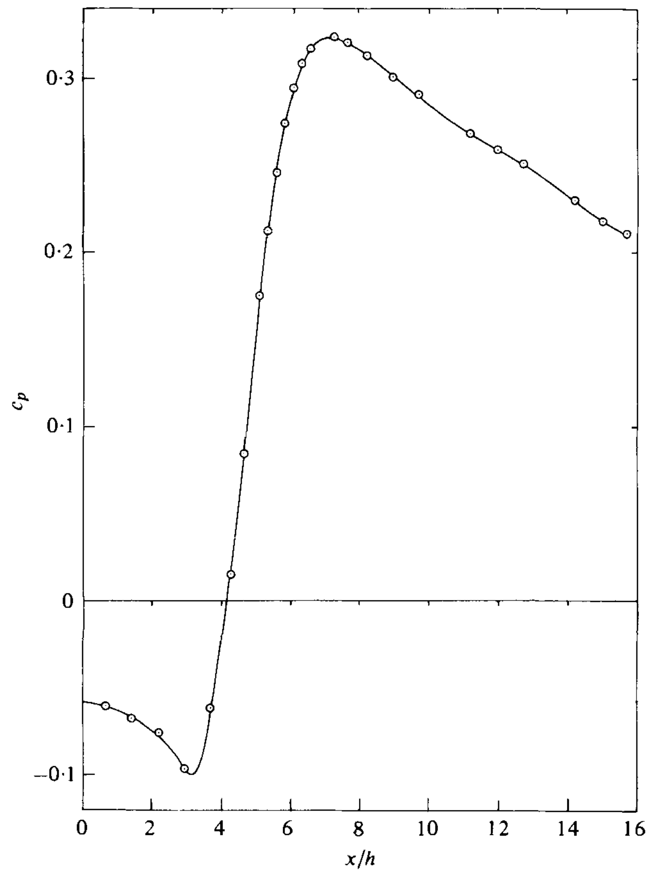

FIGURE 2. Surface pressure distribution: $c_p = (p - p_{\mathrm{ref}})/\frac{1}{2}\rho U^2_{\mathrm{ref}}$.

tubes, but Preston tubes were not used in the step flow because we anticipated that the logarithmic law would not be obeyed near the reattachment point.

Turbulence measurements were made with Disa 55D01 constant temperature anemometers with 55P01 single wire probes and 55P51 cross wire probes. Only u and v component fluctuations were measured. The anemometer outputs were linearized by Disa 55D10 linearizers before recording on analogue magnetic tape with a bandwidth of 20 kHz, and the analogue tapes were later transcribed to digital tape, using the system described by Weir & Bradshaw (1974), for subsequent processing on the Imperial College CDC computers. Because velocity measurements in the recirculation zone were expected to be inaccurate, a mean streamline was located in the potential flow by tracing the hot wake of a nichrome wire, and V-component velocities were deduced by integrating the continuity equation downward from this streamline. Further details of the test rig and apparatus are given by Chandrsuda (1976).

Figure 1 shows the flow configuration, the reference streamline, and the reattachment point, the latter being about 5·9 step heights downstream of the step as deduced from surface oil-flow measurements. (Reattachment distance is well known to be sensitive to initial conditions, but if the mixing layer becomes approximately self-

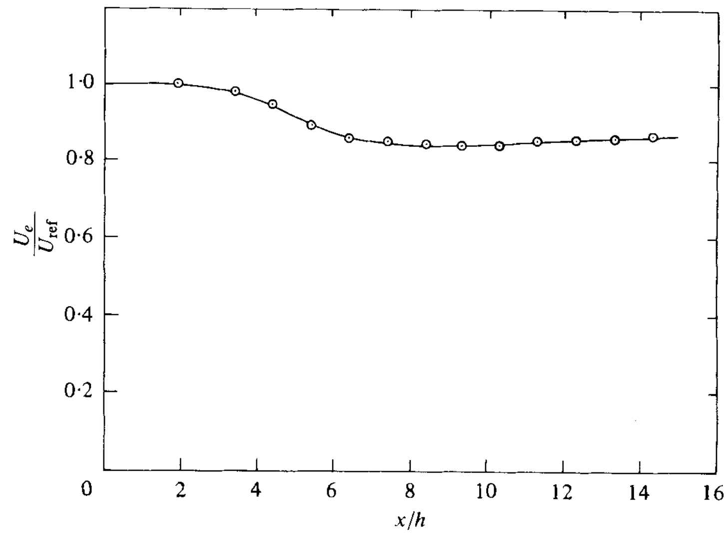

FIGURE 3. Streamwise variation of external-stream velocity at y/h = 1·8 (closely equal to velocity on 'reference streamline' in figure 1).

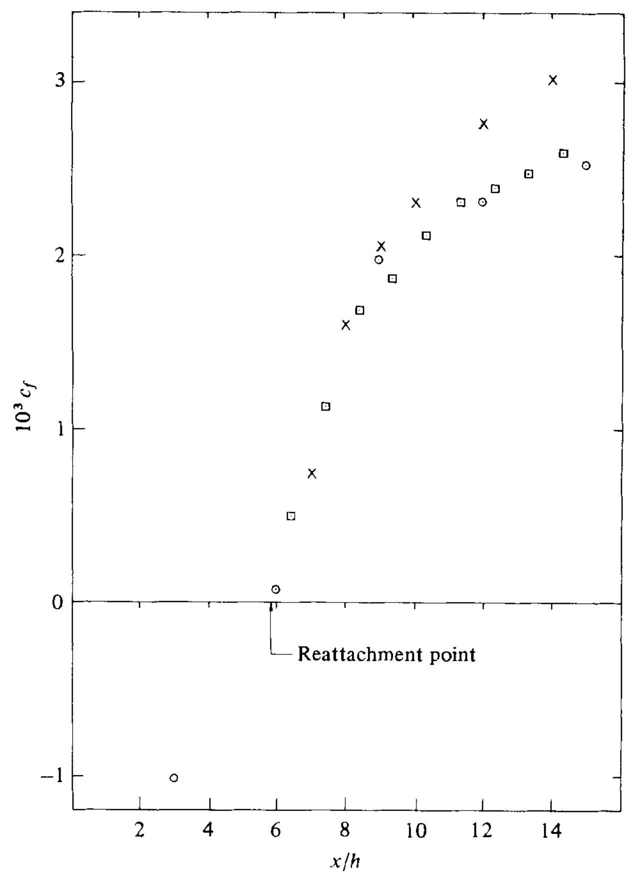

FIGURE 4. Skin-friction coefficient. ⊙, surface 'tube' results. ⊡, deduction from mean velocity profiles assuming standard logarithmic law. ×, Bradshaw & Wong (1972) (different downstream boundary condition).

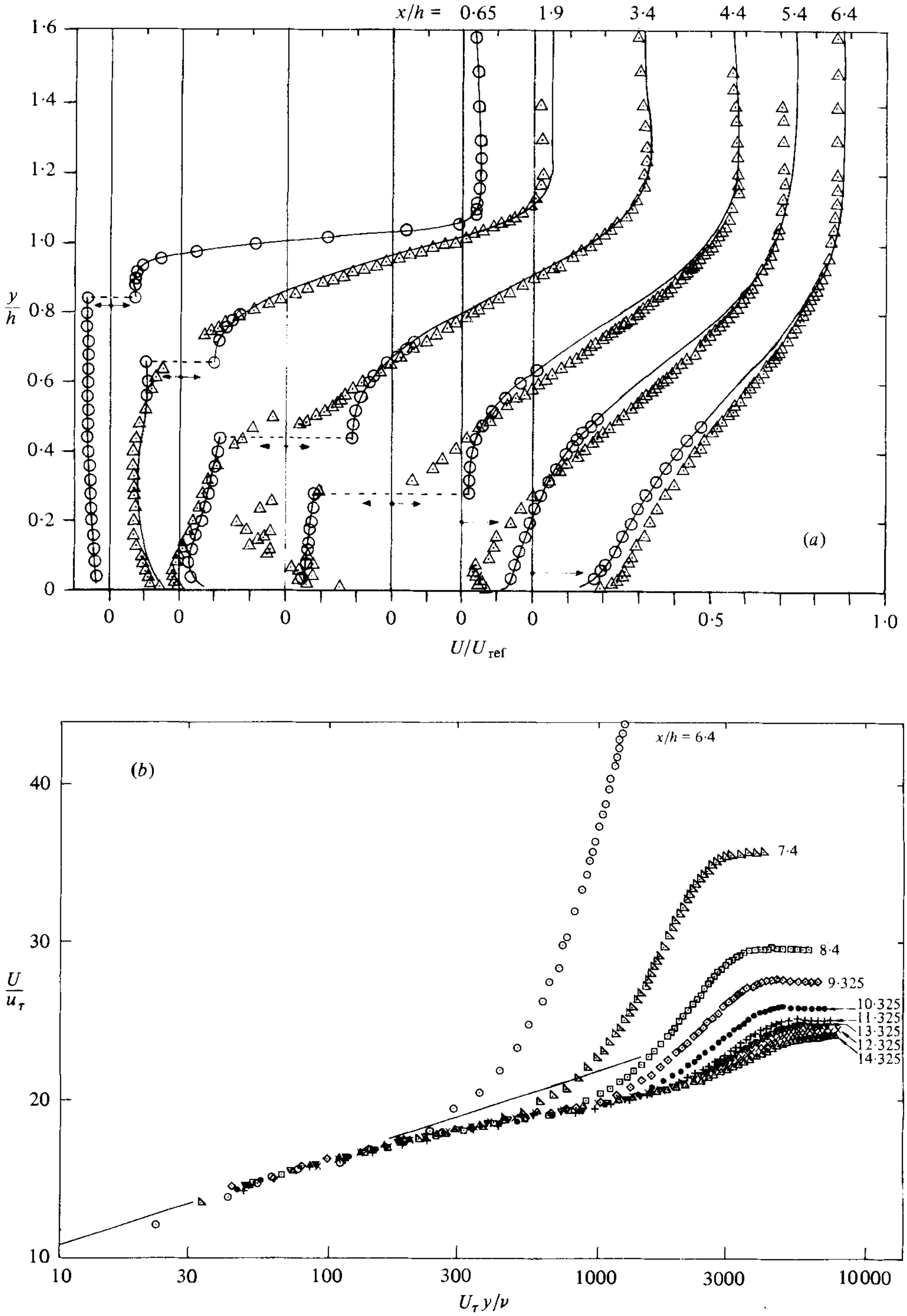

FIGURE 5. Mean velocity profiles. (*a*) Upstream of reattachment: △, pressure-probe results; —○—, hot-wire results (some points omitted for clarity); (*b*) Downstream of reattachment (pressure probe results): logarithmic scale of y. ——, 'universal' logarithmic law $U/u_\tau = (1/0{\cdot}41)\ln(u_\tau y/\nu) + 5{\cdot}2$.

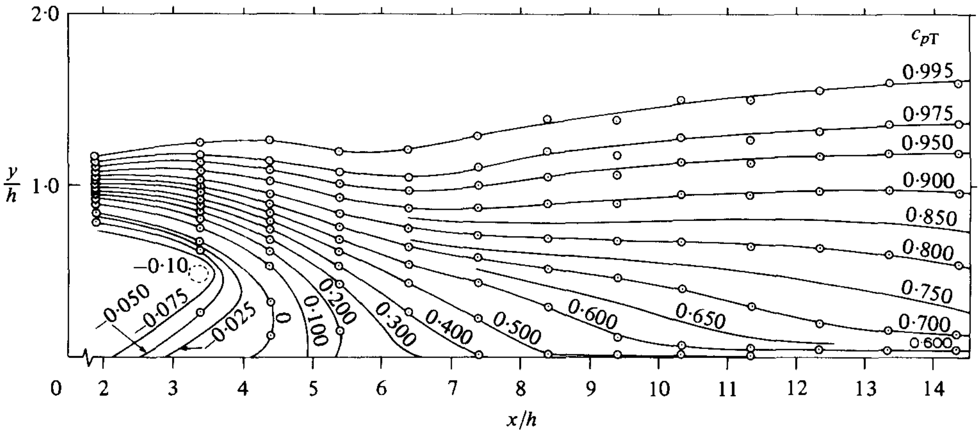

FIGURE 6. Total-pressure contours; values of $(P - p_{ref})/\frac{1}{2}\rho U_{ref}^2$.

preserving before reattachment, as in the present case, the effect of initial conditions is almost equivalent to a shift in the effective origin of the flow – that is, of the step position.) Figure 1 also gives an indication of the region in which hot-wire measurements are likely to be untrustworthy. The discussions by Hinze (1959), Bradbury (1965), Rodi (1971), Castro (1973) and di Gesso (1975) lead to the conclusion that hot-wire measurements are likely to be reliable only if the ratio of r.m.s. u-component intensity to mean velocity is less than about 0·3, while if the relative intensity exceeds 0·5 hot-wire results are likely to be highly unreliable. Results within the band of relative intensity 0·3–0·5 should be treated with caution. The line labelled $\gamma = 0{\cdot}5$ in figure 1 is the line on which the flow is turbulent for 50 per cent of the time; further details of the intermittency factor γ are given in figures 12 and 13.

3. Results

The streamwise distribution of surface pressure is shown in figure 2 and the streamwise variation of external stream velocity at a distance of 1·8 step heights above the surface is shown in figure 3; the overall decrease in external stream velocity suggests that the roof angle chosen to simulate infinite-stream conditions was somewhat too small, but the measurements are still usable as a test case by prescribing boundary conditions on the tunnel roof, or the reference streamline on which the velocity should be negligibly different from that given in figure 3. The correlation of reattachment distance with roof height by Kuehn (1980) implies that the roof inclination was slightly too *large* but the difference between the correlation and the present results is within the scatter of the data used by Kuehn. The pressure distribution collapses fairly well on the generalized co-ordinates of Roshko & Lau (1965) up to a distance of about $1{\cdot}5x_r$, as shown by Chandrsuda (1976).

Skin-friction measurements using the surface tube are plotted in figure 4, together with values deduced from the mean velocity profiles on the assumption that the standard logarithmic law applies *near the surface*; the two seem to agree fairly well, and the mean velocity profiles plotted on semi-logarithmic axes in figure 5(*b*) confirm that the logarithmic law is fairly well obeyed up to a height of at least 0·1 step

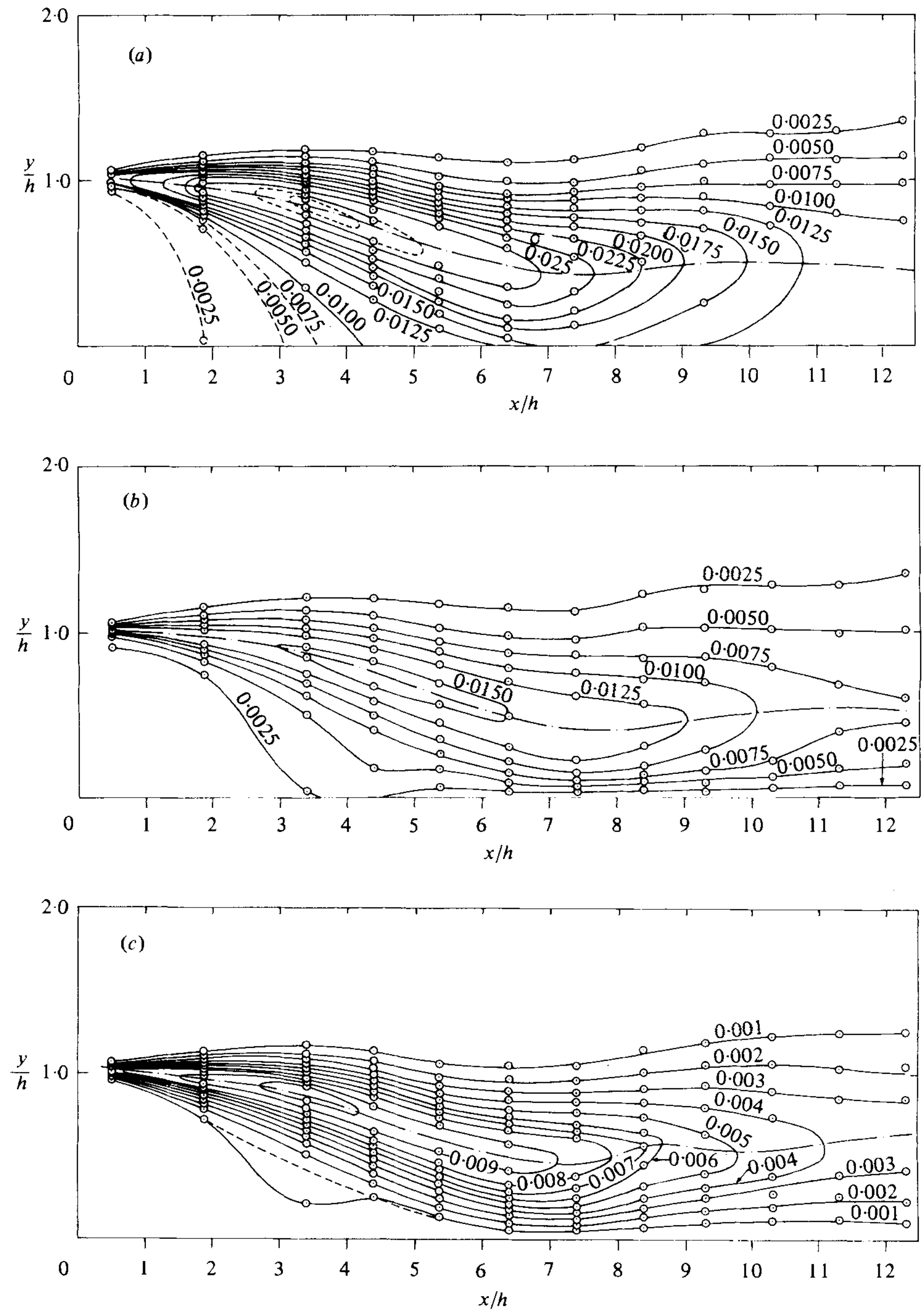

FIGURE 7. Reynolds stress contours made dimensionless by ρU_{ref}^2. Dotted contours are conjectural: chain-dotted lines are loci of maximum intensity. (*a*) Longitudinal normal stress $\overline{u^2}$; (*b*) vertical normal stress $\overline{v^2}$; (*c*) shear stress $-\overline{uv}$.

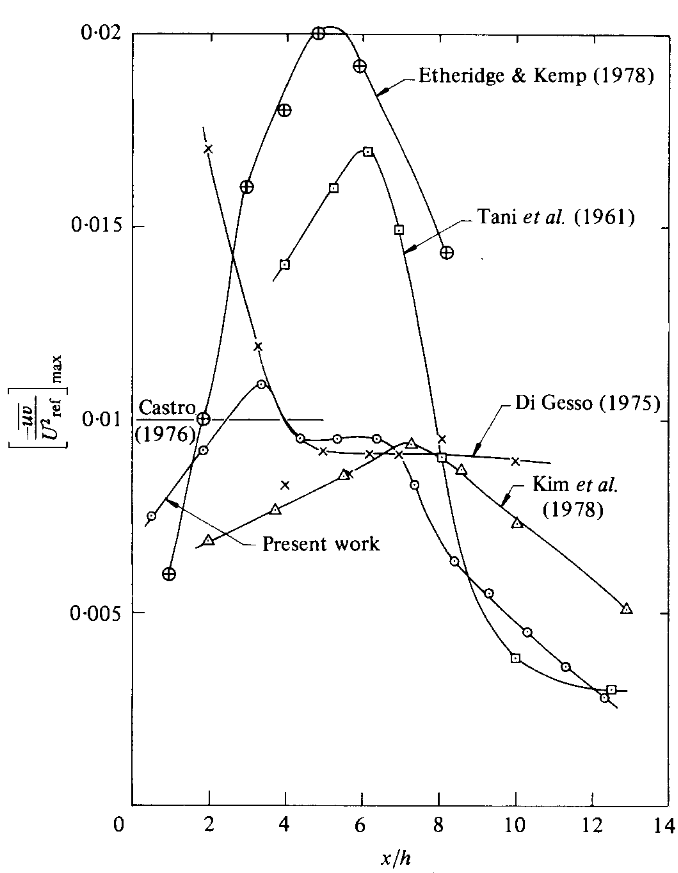

FIGURE 8. Maximum shear stress compared with results of other workers. Castro results are for a plane mixing layer in same wind tunnel as present work.

heights from the surface, even very close to reattachment. Figure 5(*a*) shows mean velocity measurements with pressure probes and with hot wires, and it is seen that except in the recirculating region, the results are in tolerably good agreement. The sign of the velocity indicated by the hot wire has been changed where necessary to agree with the Pitot-tube results, and the Pitot-tube traverses are composites of results obtained with forward-facing and rearward-facing tubes. The pressure probe results are used in figure 5(*b*), being less scattered. Chandrsuda (1976) gives the static pressure profiles used in deducing the results of figure 5. The maximum pressure difference across the shear layer is only about 0·06 of the reference dynamic pressure, and occurs near the reattachment point. As usual in flows with varying static pressure, the total pressure is a more meaningful variable than the velocity, and the total-pressure coefficient $(P-p_{ref})/(P_{ref}-p_{ref})$ is contour-plotted in figure 6, on the same scale as figure 1. The shear-layer edge $y = \delta$ is defined here as the position at which the total-pressure coefficient is 0·99, corresponding, if the static pressure variation across the layer is negligible, to the standard definition of δ_{995}: ($\sqrt{0{\cdot}99} \doteq 0{\cdot}995$).

Reynolds-stress measurements at different downstream positions are plotted in figure 7. The general level of turbulence intensity rises slightly with increasing

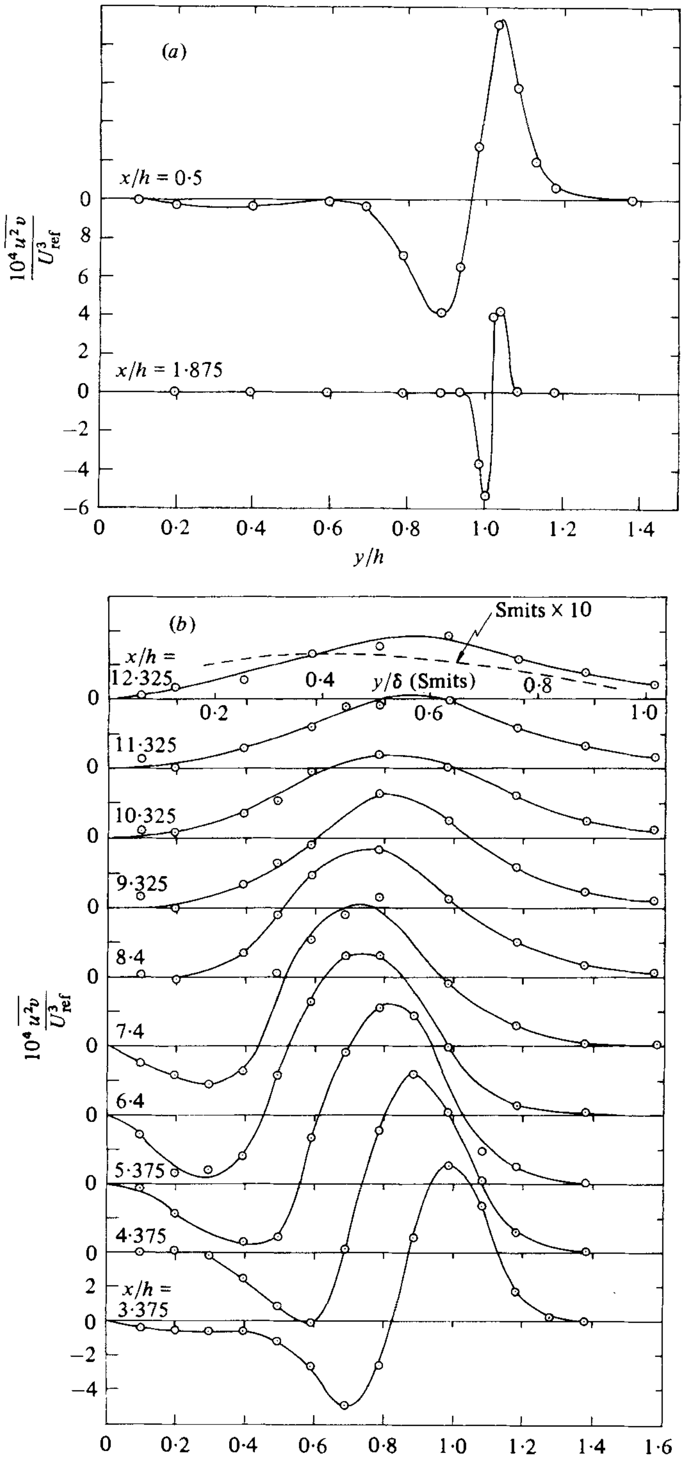

FIGURE 9. Triple product u^2v. Ordinate scale shown for lowest curve, other scales displaced upwards, with zeros as shown. Dotted line from constant-pressure boundary layer results of Smits *et al.* (1979), $U_e\theta/\nu \approx 5000$, magnified tenfold and plotted against y/δ. (*a*) $x/h = 0{\cdot}5$, $1{\cdot}875$. (*b*) $x/h = 3{\cdot}375$ to $12{\cdot}325$.

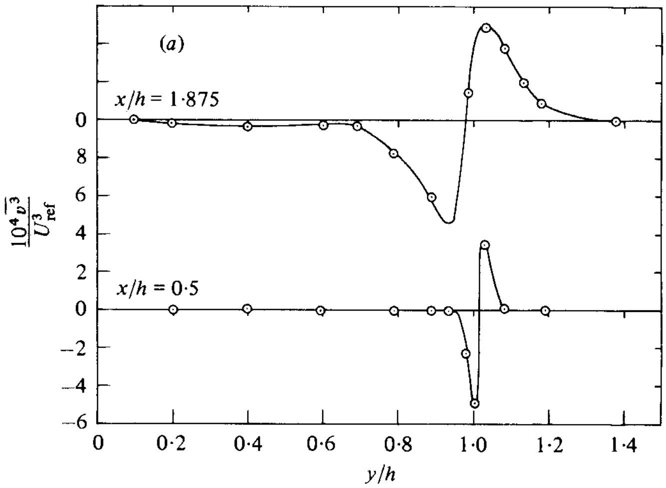

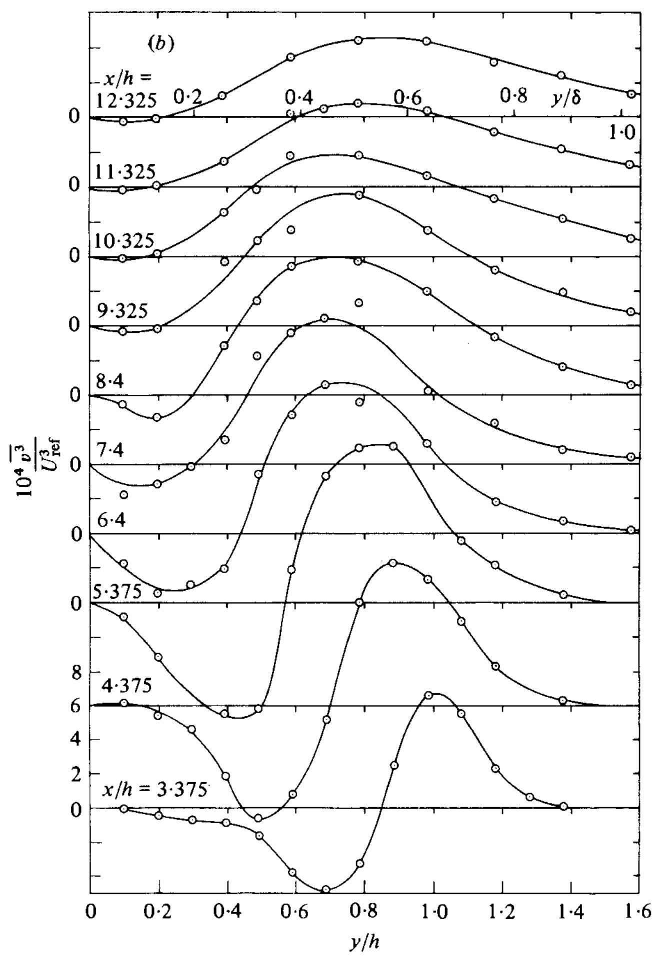

FIGURE 10. Triple product $\overline{v^3}$: details as in figure 9. (a) $x/h = 0{\cdot}5$, $1{\cdot}875$. (b) $x/h = 3{\cdot}375$ to $12{\cdot}325$.

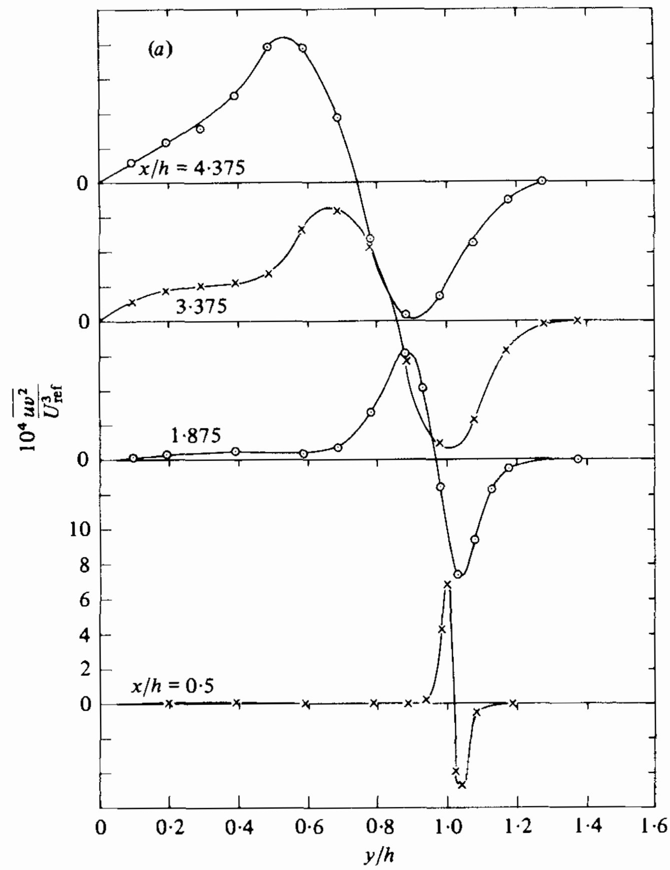

FIGURE 11. Triple product $\overline{uv^2}$: details as in figure 9. (a) x/h = 0·5 to 4·375. (b) x/h = 5·375 to 12·325.

downstream distance up to the reattachment point (we do not expect the flow to be exactly self-preserving), and then decreases rather spectacularly, by more than a factor of 2 on mean square between x/h = 6·4 and 12·3. As will be seen later, the shear correlation coefficient also decreases, though less spectacularly. Contour plots of the Reynolds stresses are given by Chandrsuda (1976). Figure 8 shows the maximum shear stress plotted against downstream distance, compared with the results of other workers: the large differences between different data sets will be discussed later. Figures 9 to 11 show the triple products $\overline{u^2v}$, $\overline{v^3}$ and $\overline{uv^2}$; Chandrsuda gives values of $\overline{u^3}$ as well, but the results can be summarized by saying that the u-component skewness is almost equal to the v-component skewness except near the outer edge of the shear layer.

The intermittency factor is plotted in figures 12 and 13. The results were obtained by applying thresholds to the first and second time derivatives of uv, as described by Murlis (1975), and, like Murlis' results, the measurements asymptote to about 0·9 instead of unity. The discussion by Murlis, Tsai & Bradshaw (1980) suggests that a tolerably accurate intermittency factor could be obtained by factoring the present results uniformly so that the maximum value reached unity; the actual maximum

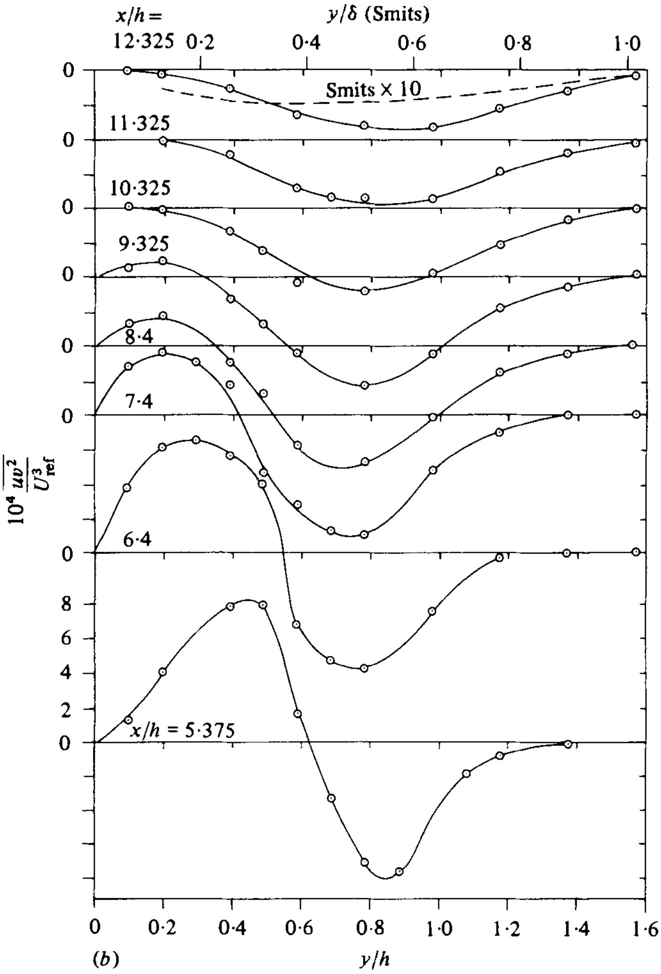

FIGURE 11 (b). For legend see p. 182.

value in a free mixing layer is negligibly smaller than unity. Further derived results are given below. Data from the experiment are available in machine-readable form from Thermosciences Division, Stanford University, as part of the data bank for the 1980–81 Conference on Complex Turbulent Flows.

4. Discussion

4.1. *The mean flow*

The logarithmic plots of mean velocity profiles in figure 5 (b) show the dip below the standard logarithmic law which Bradshaw & Wong (1972) showed to persist to a downstream distance of about fifty step heights. The reason is that the existence of the standard logarithmic law is normally proved by assuming the length scale of the flow is proportional to y, while at, and just downstream of, reattachment the length scale will be roughly constant, as it is in a free mixing layer, except near the surface. Qualitative use of mixing-length arguments shows that a larger length scale implies

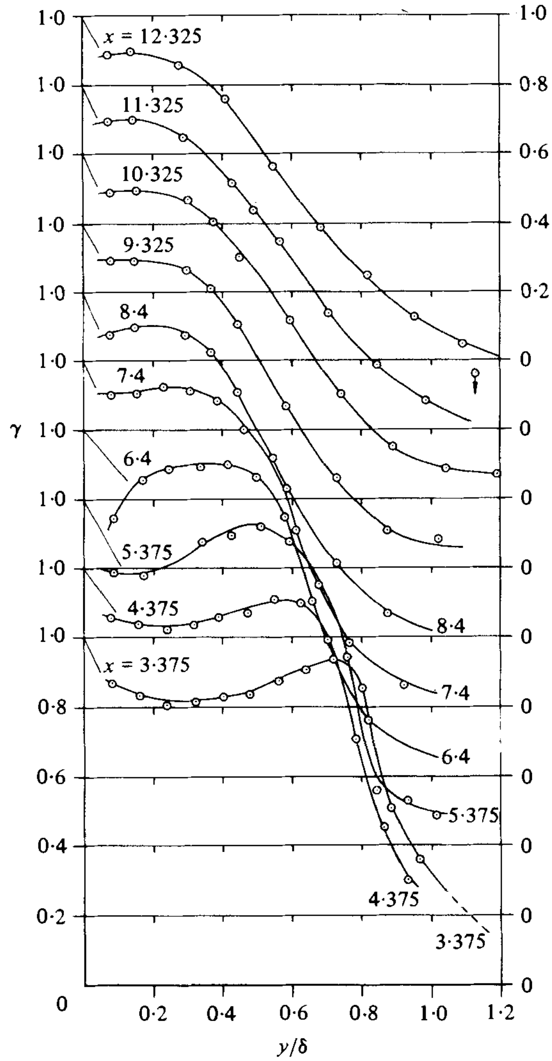

FIGURE 12. Intermittency, plotted against y/δ_{995}. The $\gamma = 0{\cdot}5$ contour is shown on figure 1.

a smaller velocity gradient for a given shear stress – that is, a dip below the logarithmic law. The persistence of the dip implies the persistence of the abnormally large length scale. The mean velocity profiles upstream of reattachment are undoubtedly inaccurate in the recirculating region (although the tolerable correspondence between hot-wire and Pitot-tube results except very near the zero-velocity point suggest that the results are of better-than-qualitative use). The maximum reversed flow velocity, reached at 3–4 step heights downstream of the step, is roughly 0·3 of the reference velocity. Skin-friction measurements (figure 4) with the surface tube could be made only at fixed insertion locations on the tunnel floor, but the one point in the separated region shows a skin friction coefficient of about 0·3 of the typical downstream-going value. Thus, the measurements confirm the modern view that the separated region can certainly not be regarded for calculation purposes as a 'dead water' area.

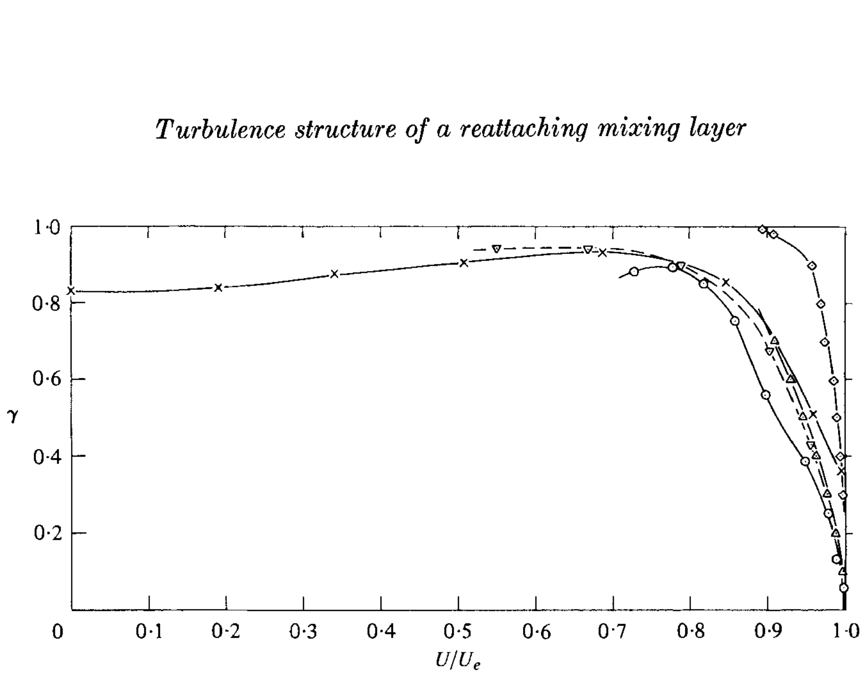

FIGURE 13. Intermittency as a function of mean velocity in various shear layers. Step flow (present results): —×—, x/h = 3·375; —○—, x/h = 12·325. Step flow (Bradshaw & Wong 1972); —△—, x/h = 30. Plane mixing layer (Castro & Bradshaw 1976): - - -▽- - -. Constant-pressure boundary layer (Klebanoff 1955): —◇—.

4.2. *The Reynolds stresses*

The Reynolds-stress measurements upstream of reattachment show maximum values similar to those found by Castro & Bradshaw (1976) in a plane mixing layer, when normalized on U_{ref}. It is of course arguable that the normalization velocity in the present case should be the maximum velocity difference across the layer, which is as much as $1{\cdot}3U_{\text{ref}}$, but it is doubtful whether the concentrated and highly unsteady reversed flow affects the mixing layer in the same way as a uniform external stream. The u and v component intensities both rise to values ten or fifteen per cent above those of Castro & Bradshaw, while the maximum shear stress is closely equal to that of Castro & Bradshaw. Bradshaw (1966) suggested that a rough criterion for full development was $x > 1000\theta_0$, or $x/h > 4$ in the present case. The best evidence of full development, in the present experiments, is that the maximum shear stress reaches a roughly constant value by $x/h = 4$, before falling rapidly after reattachment. Figure 8 shows that di Gesso's mixing layer took a rather long time to reach full development, and it is not clear why his shear stress did not decrease after the reattachment. The shear stress measured by Tani, Iuchi & Komoda (1961) behind a step with a rather thick boundary layer reaches a very high value before descending steeply to join the present results fairly soon after reattachment; Tani's u component measurements agree somewhat better with the present data. Eaton & Johnston also review step flows in general and streamwise development of Reynolds stresses in particular. They emphasize the large effect of initial conditions on Reynolds stress and on reattachment distance (Brederode 1975 found that x_r/h increased from 5·25 to 6·0 when the initial boundary layer was tripped). Reattachment distance is directly affected by pressure gradient (as discussed by Kuehn) and the flow distortion near reattachment clearly has a large effect on Reynolds stresses, so that the scatter in figure 8 comes partly from differences in initial conditions, partly from differences in boundary conditions (imposed pressure gradient).

x/h	1·875	3·375	4·375	5·375	6·4	7·4	8·4	9·325	10·325	11·325	12·325
$\bar{Y}/\delta_{995}$	0·96	0·885	0·770	0·77	0·66	0·61	0·55	0·56	0·60	0·60	0·59
δ_{995}/h	1·18	1·26	1·27	1·20	1·22	1·30	1·40	1·38	1·5	1·52	1·56
Y/h	1·13	1·11	1·11	0·98	0·92	0·79	0·77	0·77	0·90	0·91	0·92
τ at $\bar{Y}$	0·0013	0·0024	0·0043	0·0035	0·0048	0·0048	0·0048	0·0042	0·0030	0·0027	0·0027
R_{12} at τ_{max}	0·49	0·51	0·44	0·46	0·47	0·46	0·42	0·40	0·38	0·40	0·39

TABLE 1. Height of half-intermittency point $\bar{Y}$, shear stress at $\bar{Y}$ and shear correlation coefficient $R_{12} = -\overline{uv}/(\overline{u^2}\,\overline{v^2})^{\frac{1}{2}}$ at position of maximum shear stress.

For the present measurements, table 1 shows the variation of maximum shear stress, the shear correlation coefficient at the position of maximum shear stress, and the shear stress at the position where $\gamma = 0{\cdot}5$; the last-named variable was chosen as a quantity that should be constant in the outer region of a self-preserving flow. The shear correlation coefficient R_{12} rises to a value of about 0·47 in the 'fully developed' mixing layer, and then falls to about 0·4 after reattachment, with no sign of recovery towards the usual fully developed boundary-layer value of about 0·45 to 0·5. The percentage decrease in R_{12} is very much smaller than that in shear stress, but shows that the intensities decrease slightly more slowly than the shear stress does. The shear stress at the point where $\gamma = 0{\cdot}5$, the average position of the instantaneous turbulent/non-turbulent boundary, remains roughly constant until about $x/h = 9$, falling thereafter and apparently asymptoting to about 0·6 of the 'fully developed' value. The 'asymptotic' value is still rather larger than a typical surface shear stress in a constant pressure boundary layer, so that a further slow decrease towards the much smaller boundary-layer value is inevitable. The reasons for the collapse in turbulence intensity will be discussed in relation to the energy-balance evaluation below.

4.3. *The triple products*

The triple products in figures 9–11 also show spectacular changes after reattachment. In a plane mixing layer all three are roughly antisymmetrical about the mixing-layer centre-line, and the same behaviour is seen here, upstream of reattachment. Triple products in the rather chaotic reversed flow appear to be small, as one would expect; since triple products are extremely sensitive to nonlinearity of hot-wire response, this gives one *some* confidence in the accuracy of the triple product results in high-intensity regions. At or just before reattachment the excursion of the triple product on the side nearer the surface decreases very rapidly in all cases, and by $x/h = 10$ the profiles of the triple products tend monotonically to nearly zero at the wall. Now negative values of $\overline{u^2v}$, say, imply that on the average eddies with large (u component) fluctuations move towards the wall, away from the region of maximum intensity at roughly $x/h = 0{\cdot}8$. It is known that the main contribution to the triple products come from the large eddies, and their rapid attentuation near the wall can be attributed to the effect of the boundary condition $v = 0$ on the large eddy structure. It is sometimes helpful to think of this constraint as being applied by an instantaneously equal image turbulent flow in the half-space $y < 0$. Clearly, the effect of the wall will be transmitted by pressure fluctuations, rather than by eddy migration alone, and it is not meaningful to enquire about the rate at which the effect spreads out from the wall; in fact the peak positive value of $\overline{u^2v}$ (for instance) also starts to decrease more or less at the reattachment point. The effect of the boundary condition $u, w = 0$ at the solid surface spreads outwards by vorticity diffusion rather than by pressure fluctuations. Thomas & Hancock (1977) show that the effect of the constraint on the tangential component of turbulent motion is negligible, at high Reynolds numbers, compared with the constraint on the normal component fluctuation. In the present case the effect of the constraint $u = 0$ is to cause an internal boundary layer to grow out from the surface, but figure 6 shows that the streamwise total-pressure gradient near the surface is very small indeed downstream of reattachment; the thickness of the region in which the velocity profile follows the standard logarithmic law is likely to be an underestimate of the thickness of the internal layer, but it is significant that (figure 5) this boundary stays roughly constant at $u_\tau y/\nu = 100$ throughout the region of measurement. Antonia & Luxton (1972) found a similar very slow growth of the internal layer downstream of a change from large to small surface roughness; indeed their flow has many points of qualitative similarity with the present experiment, both being examples of highly turbulent flows encountering boundary conditions for which the self-preserving flow is only weakly turbulent (i.e. a constant pressure smooth surface boundary layer). It is noteworthy that, although the streamwise decrease of triple products in the outer part of the shear layer roughly follows the decrease in shear stress or shear-stress gradient, the decrease of triple products near the surface is far more rapid than the decrease of shear-stress or intensity gradient with streamwise distance; that is, the presence of the solid surface has a marked effect on the apparent gradient diffusivity of intensity or shear stress, and throws doubt upon the usefulness of gradient diffusivity even as a pragmatic means of correlating experimental data. At the last measurement station, $x/h = 12{\cdot}3$, the triple-product profiles are roughly the same shape as in a boundary layer but typical values are larger, by a factor of 10 or more, than in a boundary layer with the same free-stream velocity.

The intermittency measurements (figure 12) are unremarkable, at least if they are factored to give maxima of unity as discussed in §3. Chandrsuda (1976) shows that the direct measurements presented here agree fairly well with an intermittency defined as the minimum value of u-component flatness factor on a given profile, divided by the local value. Values of intermittency in the reversed flow are not very meaningful; on any normal definition of intermittency they should be unity. The plots of intermittency against mean velocity in figure 13, thought to be the simplest method of comparing results for different types of shear layer, show that upstream of reattachment the present mixing-layer results agree fairly well with the standard mixing-layer results of Castro & Bradshaw, while downstream of reattachment the intermittency at a given velocity ratio decreases further, although it must eventually rise to the boundary-layer curve. The measurements at $x/h = 30$ by Bradshaw & Wong were made by a slightly different digital technique to that used in the present work, but undoubtedly show that the relation between intermittency and velocity is still more typical of a mixing layer than of a boundary layer even at this large distance downstream of reattachment. The standard deviation of the intermittency interface position increases rather rapidly *after* reattachment, but there is no real evidence of the large increase in the reattachment region that would be expected if large eddies moved alternately upstream and downstream at reattachment.

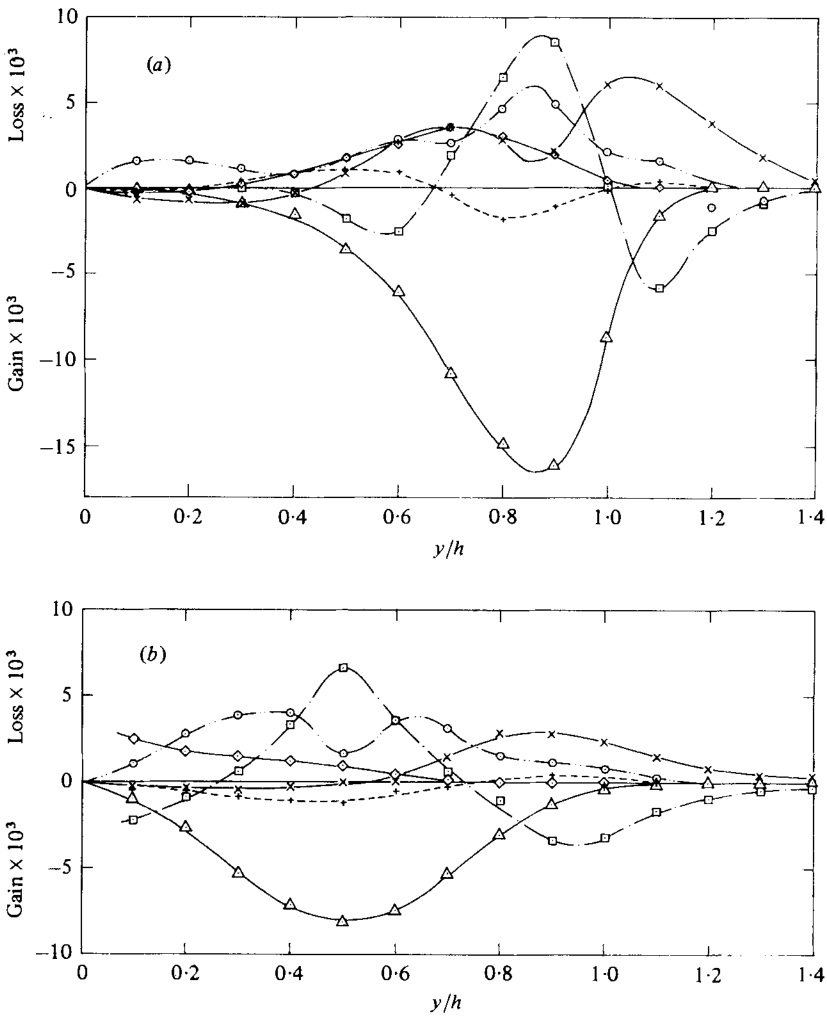

FIGURE 14. Turbulent energy balance; all terms made dimensionless by U_{ref}^3/h. Turbulent energy $\frac{1}{2}(\overline{u^2}+\overline{v^2}+\overline{w^2})$ approximated by $\frac{3}{4}(\overline{u^2}+\overline{v^2})$; dissipation by difference; pressure diffusion neglected. Results unreliable in high-density region near surface (see figure 1). ×, advection; △, production by shear stress; ◇, production by normal stress; ⊡, transverse diffusion; +, longitudinal diffusion; ○, dissipation. (*a*) $x/h = 3{\cdot}4$; (*b*) $x/h = 6{\cdot}4$; (*c*) $x/h = 8{\cdot}4$; (*d*) $x/h = 11{\cdot}3$.

Several investigators (e.g. Kim, Kline & Johnston 1978) have suggested this behaviour on the strength of surface tuft measurements: however, reversals of the slow-moving flow near the surface are not incompatible with splitting, rather than alternation, of large eddies further from the surface as suggested by Bradshaw & Wong.

4.4. *Energy and shear-stress balances*

Figures 14 and 15 show balances of the turbulent kinetic energy, approximated by $\frac{3}{4}(\overline{u^2}+\overline{v^2})$, and figure 16 shows shear stress balances at the same streamwise positions;

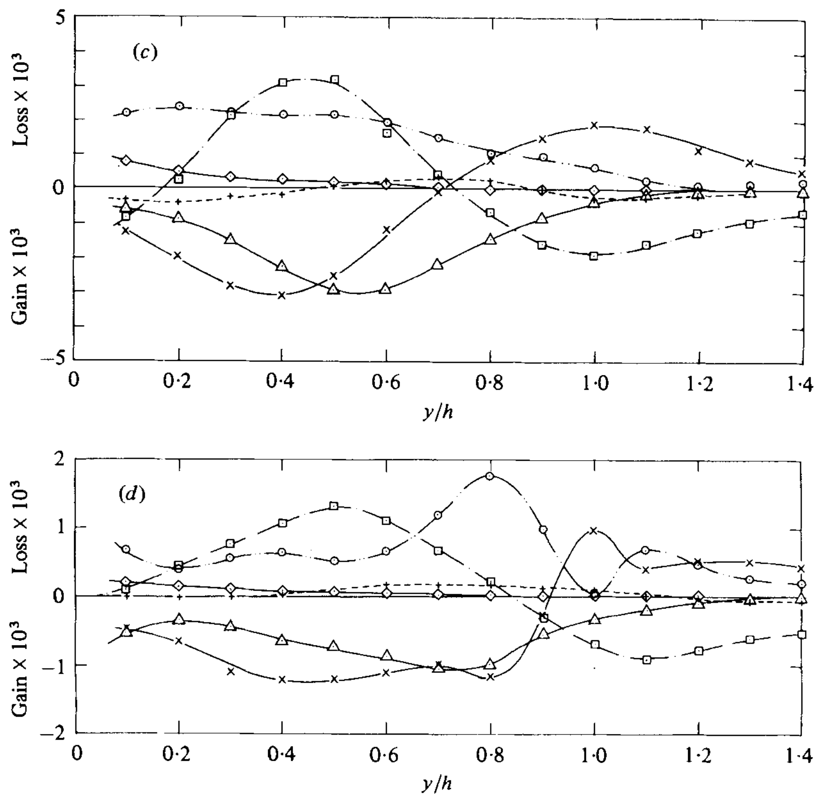

FIGURE 14 (*c*, *d*). For legend see p. 188.

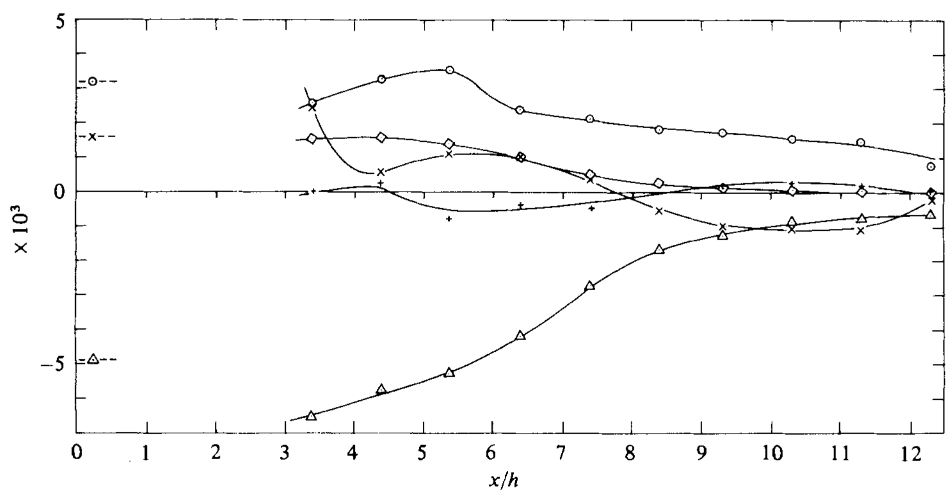

FIGURE 15. Integrals of energy-balance terms, made dimensionless by U^3_{ref}. ×, advection; △, production by shear stress; ◇, production by normal stress; +, longitudinal diffusion, ○, dissipation (by difference). Points at left are results of Castro & Bradshaw (1976) for plane mixing layer.

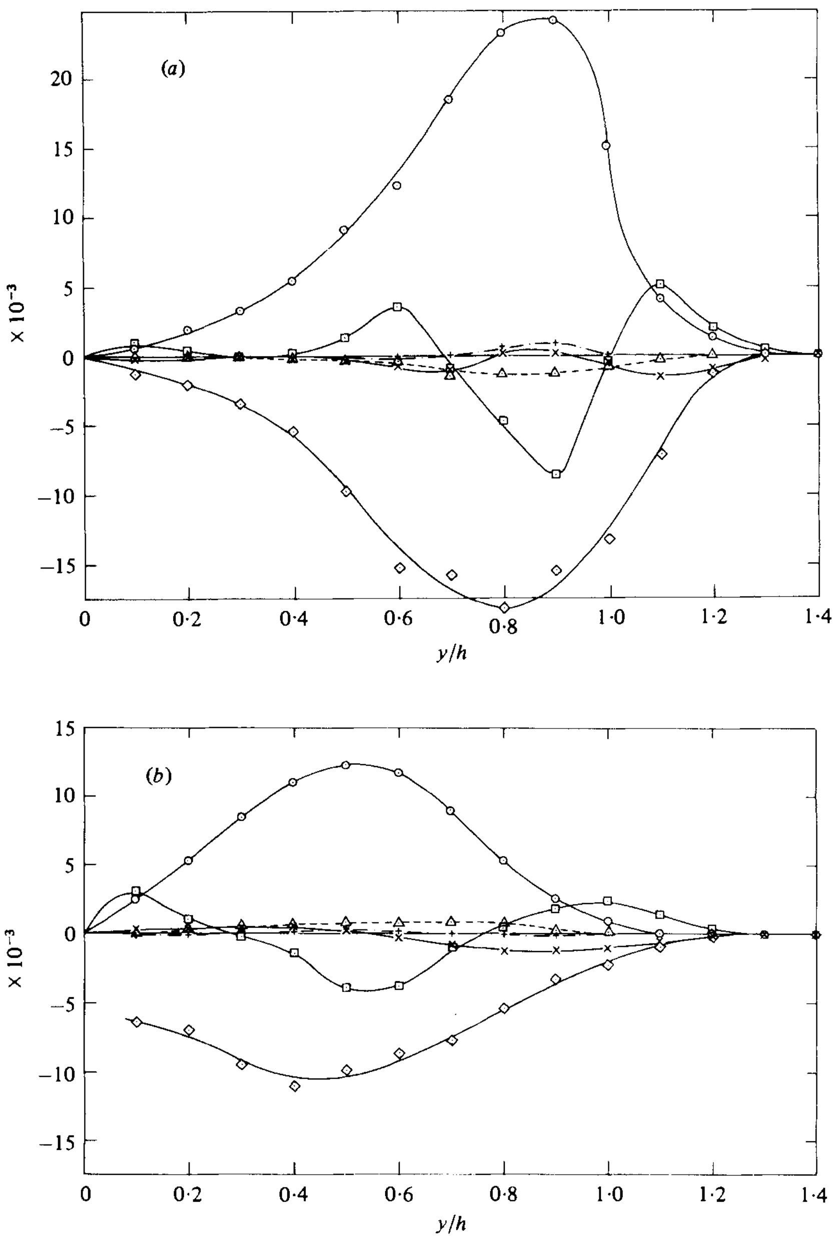

FIGURE 16. Shear-stress balance; all terms made dimensionless by U^3_{ref}/h. ×, mean transport; ○, $\overline{v^2}\,\partial U/\partial y$ generation; △, $\overline{u^2}\,\partial V/\partial x$ generation; ⊡, transverse turbulent transport; +, longitudinal turbulent transport; ◇, pressure-strain redistribution. (a) $x/h = 3{\cdot}4$; (b) $x/h = 6{\cdot}4$; (c) $x/h = 8{\cdot}4$; (d) $x/h = 11{\cdot}3$.

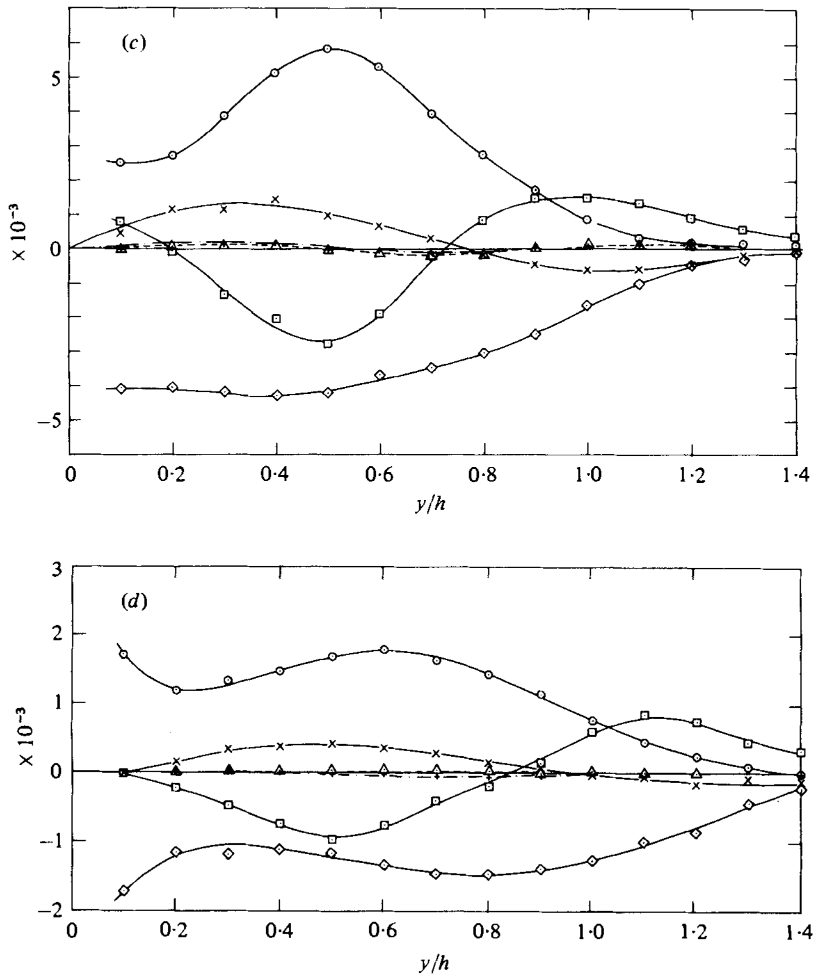

FIGURE 16 (*c*, *d*). For legend see p. 190.

more detailed results are given by Chandrsuda (1976). The terms have been evaluated in x, y co-ordinates from the equations

$$\frac{D}{Dt}(\tfrac{1}{2}\overline{q^2}) = -\overline{uv}\frac{\partial U}{\partial y} - (\overline{u^2}-\overline{v^2})\frac{\partial U}{\partial x} - \frac{\partial}{\partial x}\left(\left[\frac{\overline{p'u}}{\rho}\right] + \tfrac{1}{2}\overline{q^2u}\right) - \frac{\partial}{\partial y}\left(\left[\frac{\overline{p'v}}{\rho}\right] + \tfrac{1}{2}\overline{qv}\right) - \epsilon, \quad (1)$$

$$\frac{D}{Dt}(-\overline{uv}) = \overline{v^2}\frac{\partial U}{\partial y} + \overline{u^2}\frac{\partial V}{\partial x} - \overline{\frac{p'}{\rho}\left(\frac{\partial u}{\partial y} + \frac{\partial v}{\partial x}\right)} - \frac{\partial}{\partial x}\left(\left[\frac{\overline{p'v}}{\rho}\right] + \overline{u^2v}\right) - \frac{\partial}{\partial y}\left(\left[\frac{\overline{p'u}}{\rho}\right] + \overline{uv^2}\right), \quad (2)$$

transport by pressure fluctuations (terms in brackets) being neglected.

Longitudinal diffusion and normal stress production are significant in the region upstream of reattachment where the mixing layer is significantly inclined to the axes, and also in restricted regions downstream of reattachment. Well upstream of re-attachment the results are tolerably close to those of Castro & Bradshaw (see also Castro 1973, where the plane-layer results are plotted in detail), the transverse diffusion of turbulent energy being roughly one half of the total production rate.

Values of dissipation, evaluated as the difference of all the other terms, rely rather heavily on accuracy of estimates of triple product gradients to evaluate the transverse diffusion term, and obvious eccentricities occur in figure 14 although the integral of the dissipation across the shear layer (figure 15) is plausible except perhaps at the last station where streamwise gradients are difficult to evaluate. The shear stress balance again agrees fairly well with Castro's, and, because transverse turbulent transport is a smaller fraction of the generation term than in the case of the energy balance, the pressure strain term deduced by difference is acceptably well behaved. (It is known that the pressure strain term has two parts, one dependent on the mean velocity gradient, which opposes the generation term and should strictly be grouped with it, and another part which represents 'scrambling', akin to dissipation of turbulent energy; reassignment of the pressure strain term in this way would make the shear stress balance look much more like the turbulent energy balance, but is not of course practicable.)

The quantities plotted in figures 14 and 16 are made dimensionless by U^3_{ref}/h, and therefore decrease with increasing distance downstream even in a fully developed mixing layer. However, the dissipation in the inner part of the flow decreases much less rapidly than the production term near and downstream of reattachment; at $x/h = 4{\cdot}4$, the maximum dissipation (drawing a smooth curve through the variation shown) is only about half the maximum production, and occurs at about the same value of y, while by $x/h = 7{\cdot}4$ the dissipation reaches a maximum significantly nearer the surface than the production and is as large as three-quarters of the maximum production. Because of the large changes in triple products mentioned earlier, the gain by diffusion on the low-velocity side of the flow has almost disappeared by $x/h = 7{\cdot}4$, although there is still a large loss from the region of maximum production. The result of the large dissipation and large loss by triple product diffusion is a rapid decrease in intensity, particularly in the region close to the surface. By the last station at which an energy balance was evaluated, $x/h = 12{\cdot}3$, turbulent energy production starts to rise near the wall but is still falling rapidly with increasing x in the main part of the layer, while transverse diffusion remains comparatively large. Note that the integrals in figure 15 would be *independent* of x in a self-preserving flow.

As might be expected, the main feature in the shear stress balances near and downstream of reattachment is a rise (in absolute terms as well as relative to the maximum value) of the pressure strain term, which precedes the rise in generation term due to the increase in turbulence intensity and velocity gradient near the wall. It is probable that this rapid rise in the pressure strain term is attributable mainly to a change in the mean strain dependent part of the term, perhaps because of the contribution of dV/dx or dU/dx to the mean strain rate near reattachment. (Recall that in Wood's mixing layer, in which dV/dx and dU/dx were very small, the Reynolds shear stress did not decrease rapidly after 'reattachment'.) The overall effect of positive dV/dx on a turbulent shear layer with positive dU/dy is to increase turbulence intensity by the destabilizing effects of streamline curvature. The effect of dU/dx could be exerted non-locally via the splitting of large eddies at reattachment, which is more likely to cause the observed decrease in Reynolds stresses than the alternative mechanism of alternate downstream and upstream deflection of large eddies at reattachment. The ratio of transverse turbulent transport to generation of shear stress increases with increasing distance downstream, though less markedly than the corresponding ratio in the turbulent energy balance results. Broadly, however, the shear stress balances help to confirm the deductions made above from the turbulent energy balances.

5. Conclusions

The mixing layer in the present experiment seems to approach as close as can be expected to self-preservation before reaching the reattachment region, in contrast to the results of previous workers. Thus the effect of initial conditions on the mixing layer, currently the subject of controversy, should be negligible at reattachment. The measurements show that the mixing layer bounding a separation bubble with a thin initial laminar boundary layer is *not* greatly different from a plane mixing layer with uniform external stream. The mixing layer begins to change rapidly only in the region near reattachment, and the main effect is confinement of the large eddies by the normal component boundary condition $v = 0$ at the solid surface, leading to a marked decrease in triple products and in the transport of turbulent energy and shear stress towards the solid surface from the region of maximum turbulent intensity. Approach to the solid surface also leads to a large increase in the pressure strain 'redistribution' term in the transport equation for turbulent shear stress, which can also be regarded, qualitatively, as a result of the confinement of the large eddies by the solid surface; a corresponding increase in turbulent energy dissipation rate in the inner half of the shear layer near and downstream of reattachment may well result from an increase in spectral energy transfer caused by distortion of the strain field of the larger eddies, but this must remain a matter of speculation. As a result of the increase in pressure strain term and dissipation, both the shear stress and turbulent intensity decrease rather spectacularly downstream of reattachment; however, it is known from the work of Bradshaw & Wong (1972) that the final decrease of the turbulent energy and shear stress to the much lower values typical of a self-preserving turbulent boundary layer takes a very long time to accomplish.

These effects of approach to a solid surface imply that any calculation method intended to deal with reattaching (and possibly separating) flows should include a fairly sophisticated model for triple products, preferably based on the triple-product transport equation. The dissipation equation should include, at the least, a 'wall-effect' term; the logic of representing the pressure strain term in the shear stress equation by a transport equation does not yet seem to have been recognized by modellers, but any algebraic form used as a model for this term should also contain an allowance for wall effect.

REFERENCES

Antonia, R. A. & Luxton, R. E. 1972 *J. Fluid Mech.* **53**, 737.

Bradbury, L. J. S. 1965 *J. Fluid Mech.* **23**, 31.

Bradshaw, P. 1966 *J. Fluid Mech.* **26**, 225.

Bradshaw, P. 1972 *Imperial College Aero. Rep.* 72–10.

Bradshaw, P. 1975 *Trans. A.S.M.E.* I, *J. Fluids Engng* **97**, 146.

Bradshaw, P. 1976 *Theoretical and Applied Mechanics* (ed. W. T. Koiter), p. 103. North-Holland.

BRADSHAW, P. 1978 *Imperial College Aero. Tech. Note* 78–105.

BRADSHAW, P. & WONG, F. Y. F. 1972 *J. Fluid Mech.* **52**, 113.

BREDERODE, V. A. S. L. 1975 Three-dimensional effects in nominally two-dimensional flow. Ph.D. thesis, Imperial College, London University.

BRYER, D. W. & PANKHURST, R. C. 1971 *Pressure Probe Methods for Determining Wind Speed and Flow Direction*. London: H.M.S.O.

CASTRO, I. P. 1973 A highly distorted turbulent free shear layer. Ph.D. thesis, Imperial College, London University.

CASTRO, I. P. & BRADSHAW, P. 1976 *J. Fluid Mech.* **73**, 265.

CHANDRSUDA, C. 1976 A reattaching turbulent shear layer in incomprehensible flow. Ph.D. thesis, Imperial College, London University. (Available on microfiche from Department of Aeronautics.)

CHRISTIANSEN, T. & BRADSHAW, P. 1981 Submitted to *J. Phys.* E.

EATON, J. A. & JOHNSTON, J. P. 1980 *A.I.A.A. paper* no. 80–1438.

ETHERIDGE, D. W. & KEMP, P. H. 1978 *J. Fluid Mech.* **86**, 545.

GAVIGLIO, J., DUSSAUGE, J. P., DEBIEVE, J. F. & FAVRE, A. 1977 *Phys. Fluids Suppl.* **20**, 179.

DI GESSO, J. A. 1975 An experimental investigation of two dimensional, separated, internal flows. Ph.D. thesis, Exeter University.

HINZE, J. O. 1959 *Turbulence.* McGraw Hill.

HUSSAIN, A. K. M. F. & ZEDAN, M. F. 1978 *Phys. Fluids* **21**, 1100.

KIM, J., KLINE, S. J. & JOHNSTON, J. P. 1978 *Thermosci. Div., Stanford Univ. Rep.* MD-37.

KLEBANOFF, P. S. 1955 *N.A.C.A. Rep.* no. 1247.

KUEHN, D. M. 1980 *A.I.A.A. J.* **18**, 343.

MURLIS, J. 1975 Ph.D. thesis, Imperial College, London University.

MURLIS, J., TSAI, H. M. & BRADSHAW, P. 1980 Submitted to *J. Fluid Mech.*

RODI, W. 1971 *Imperial College Mech. Engng Dept Rep.* ET/TN/B/10; *DISA Information* no. 17, p. 9 (1975).

ROSHKO, A. & LAU, J. C. 1965 *Proc.* 1965 *Heat Transfer and Fluid Mechanics Institute* (ed. A. F. Charwat). Stanford University Press.

SIVASEGARAM, S. 1971 *J. Roy. Aero. Soc.* **75**, 793.

SMITS, A. J., EATON, J. A. & BRADSHAW, P. 1979 *J. Fluid Mech.* **94**, 209.

SMITS, A. J., YOUNG, S. T. B. & BRADSHAW, P. 1979 *J. Fluid Mech.* **94**, 243.

TANI, I., IUCHI, M. & KOMODA, H. 1961 *Aero. Res. Inst., Univ. of Tokyo Rep.* no. 364.

THOMAS, N. H. & HANCOCK, P. E. 1977 *J. Fluid Mech.* **82**, 481.

WEIR, A. D. & BRADSHAW, P. 1974 *Imperial College Aero. Rep.* no. 74–09.

WOOD, D. H. 1980 A reattaching turbulent thin shear layer. Ph.D. thesis, Imperial College, London University.

WYGNANSKI, I., OSTER, D., FIEDLER, H. & DZIOMBA, B. 1979 *J. Fluid Mech.* **93**, 325.